

Computational Modeling of Optical Response from Excitons in a Nano Optical Medium[†]

Yuanchang Sun^{1,*}, Hiroshi Ajiki² and Gang Bao¹

¹ Department of Mathematics, Michigan State University, East Lansing, MI 48824, USA.

² Graduate School of Engineering Science, Osaka University, 1-3 Machikaneyama, Toyonaka 560-8531, Japan.

Received 4 January 2008; Accepted (in revised version) 26 May 2008

Available online 16 July 2008

Abstract. Consider a time-harmonic electromagnetic plane wave incident on a microscopic semiconductor. Inside the medium, at any given frequency ω , more than one polariton mode can arise with the same frequency but different wavenumbers due to the presence of excitons. Besides Maxwell's boundary conditions, additional boundary conditions are required to handle the multi-mode polariton. In order to model the confinement effect of excitons in the microscopic semiconductor, Maxwell's equations and the Schrödinger equation are coupled to characterize the polarization in terms of the quantum description. In the weak confinement regime, we derive a perturbed dispersive dielectric constant by taking the exciton effect into account. We also analyze and compute the optical linear response of the exciton in both one-dimensional and two-dimensional confinements. For the one-dimensional case, the existence and uniqueness of the analytical solution are established in the resonance region. A finite difference method is developed to compute the two dimensional confinement.

AMS subject classifications: 78A45, 78M20, 81V10

Key words: Nano optics, exciton, modeling.

1 Introduction

The electric and optical properties of microscopic semiconductor structures are of great interest in the design and potential device applications of such structures. The most widely studied systems of this type are the quantum well, quantum wire, and quantum

[†]Dedicated to Professor Xiantu He on the occasion of his 70th birthday.

*Corresponding author. *Email addresses:* sunyuanc@msu.edu (Y. Sun), ajiki@mp.es.osaka-u.ac.jp (H. Ajiki), bao@math.msu.edu (G. Bao)

dot, which have interesting electric and optical properties [20, 25, 26, 34]. Applications include diode lasers, amplifiers, biological sensors, detection of tumor in fluorescence spectroscopy, and making better displays (quantum dot-LED displays). An emerging research direction of nanotechnologies is to understand and study the electrodynamics of the above mentioned nano optical media.

In macroscopic electromagnetic theory of bulk media, all the variables (fields, polarization, charge and current densities...) are averaged quantities. However, when the size of medium reduces to microscopic, it is essential to consider the microscopic fields which are created by atomic electric charges in motion. In this case, the quantum mechanical description of the matter system must be studied. The motion of EM fields is described by Maxwell's equations and the motion of charged particles is governed by the Schrödinger equation. From this prospective, a great deal of research has been devoted to the study of optical responses of microscopic media. To fully characterize the interaction of atoms and photons, the quantum theory of light [10] and quantum electrodynamics (QED) must be employed. In this setting, the EM fields as well as the medium are quantized and a many-body Schrödinger equation needs to be solved in QED, hence the computation of QED seems to be a formidable task without any approximation. So far, QED has been widely used in atomic physics and quantum optics [31] where the size is smaller than microscopic. Although QED provides accurate characterizations of the fields and media of interest, the required extremely intense computation prohibits QED from many practical applications. In order to overcome the high computational cost of QED, for the microscopic medium of our interest, we present a semiclassical approach which combines the classical treatment of the EM fields and the quantum mechanical treatment of the medium. The semiclassical approach has been widely used with much success in nano optics modeling. Both Cho's microscopic nonlocal response approach [9] and Keller's local field theory [21] are semiclassical methods. In Cho's theory, the induced polarization is calculated in a nonlocal way which means the applied field $\mathbf{E}(\mathbf{r})$ at a point \mathbf{r} induces polarization $\mathbf{P}(\mathbf{r})$ not only at the same position, but also at other positions within the extent of relevant wave functions" [9]. Keller's method is similar to Cho's in building two integral equations for the EM fields and the current density. However, in Cho's approach, the transverse component of the EM fields and full Coulomb interaction among particles are included in the matter Hamiltonian while the full Coulomb interaction is not included in Keller's free Hamiltonian. Another semiclassical method is called the coherent wave approach proposed by Stahl [28]. The idea is to use interband transition amplitudes to set up the constitutive equation between the current density and electric field. It should be pointed out that a common limitation of these similar semiclassical approaches is that there are many quantum effects cannot be described by the above methods: for example, the Raman scattering and luminescence. By introducing the notion of transition polarizability, Born and Huang [7] showed one can describe the Raman scattering semiclassically, which cannot be treated by all above approaches.

In this paper, we start from Cho's nonlocal response theory. However, a different Hamiltonian is used for the Schrödinger equation. For the matter Hamiltonian (unper-

turbed Hamiltonian) only the kinetic energy and Coulomb interaction of charged particles are included, and for the matter-light interaction Hamiltonian, we take the full EM field as the external field. By introducing the electric dipole moment operator of the medium, we are able to write the matter-light interaction Hamiltonian (perturbed part) into an integral form. After these initial steps, we derive a formula for the calculation of the susceptibility. Our goal is to study the interaction of light and excitons or the optical responses from excitons in a microscopic medium. In general, excitons arise as a consequence of the interaction between the electron promoted in conduction band and the hole left behind the valence band. Excitons are the main mechanism for light emission in semiconductor at low temperature (where the chemical energy kT is less than the exciton binding energy) [13]. The interaction of excitons plays a significant role in the excited-state properties of one-dimensional system [12,32], for example, carbon nanotubes. In [6], an amazing phenomenon called electromagnetic induced transparency (EIT) was found based on intrinsic free exciton and biexciton state in CuCl. In 1988, Hanamura [15] showed theoretically that the nonlinear optical polarizability can be enhanced greatly in semiconductor microcrystallites where the exciton becomes quantized due to confinement. His calculation suggested that in case of CuCl microcrystal of size about 6.4 nanometer, an enhancement of the order of 10^4 for $\chi^{(3)}$ can be expected. Such an enhancement is clearly significant from an engineering point of view, for example, materials with a large optical nonlinearity are required for optical shutters or optical information processors [23,29,30,33].

In this paper, we show that the exciton effect may strongly enhance the optical absorption. Therefore, as the size of semiconductor is getting smaller, excitons inside are no more minor perturbation as in comparable bulk system; but actually play a very important role in defining the electric and optical properties. So we need to take the motion of the exciton into account. Usually, the motion of an exciton (electron-hole pair, or e-h) is quite different in two limiting situations characterized by the ratio of the system's size L to the effective Bohr radius a_B of the exciton in bulk material [1]. Therefore, we have two cases, **a)** $L \gg a_B$ (weak confinement regime). In this limit the size quantization of the exciton is brought about, and the e-h relative motion stays almost as in the bulk material and only the center-of-mass motion is affected by the confinement; **b)** $L \ll a_B$ (strong confinement regime). This is opposite to case **a)**, the size quantization effect of the electron and hole is much larger than the exciton effect, the energy of an e-h pair is mainly determined by the individual size quantization with a small correction due to the Coulomb interaction.

Throughout the paper, we focus on the first case, i.e., the size of confined material is assumed to be larger than the Bohr radius of the exciton. Hence, the internal structure of the exciton is assumed to be similar to that in the bulk system, but its motion is quantized due to the confinement. In addition, we choose CuCl to study the exciton confinement effect since its excitons have a relatively small Bohr radius (0.7nm) and large binding energy (190 meV) [17].

For related computational modeling of classical electromagnetic media, we refer the

reader to [2–4] for nonlinear optical media, [19,22] in the setting of waveguides, and [5,14] for general media.

This paper is organized as follows: In Section 2, we reformulate the microscopic non-local response theory [4]. We use a different Hamiltonian in the reformulation, which makes the derivation of the susceptibility tensor and dispersive dielectric function more directly. Then we consider the exciton states confinement in a microscopic CuCl slab and CuCl square, and impose additional boundary conditions at the interface. In Section 3, we present some interesting numerical results to show how the exciton affect the optical properties of the semiconductor. The paper is concluded with some general remarks in Section 4.

2 Semiclassical model

2.1 Dielectric constant

Consider microscopic Maxwell's equations in the Gaussian unit:

$$\begin{cases} \nabla \cdot \mathbf{E} = 4\pi\rho, \\ \nabla \times \mathbf{E} = -\frac{1}{c} \frac{\partial \mathbf{H}}{\partial t}, \\ \nabla \cdot \mathbf{H} = 0, \\ \nabla \times \mathbf{H} = \frac{1}{c} \frac{\partial \mathbf{E}}{\partial t} + \frac{4\pi}{c} \mathbf{j}, \end{cases} \quad (2.1)$$

where \mathbf{E} and \mathbf{H} are the electric and magnetic fields, respectively, c is the light speed, \mathbf{j} and ρ are the respective microscopic (many-body) current and charge densities.

By taking the Fourier transform of the above equations, we obtain the following frequency domain microscopic equations:

$$\begin{cases} \nabla \cdot \tilde{\mathbf{E}} = 4\pi\tilde{\rho}, \\ \nabla \times \tilde{\mathbf{E}} = \frac{i\omega}{c} \tilde{\mathbf{H}}, \\ \nabla \cdot \tilde{\mathbf{H}} = 0, \\ \nabla \times \tilde{\mathbf{H}} = -\frac{i\omega}{c} \tilde{\mathbf{E}} + \frac{4\pi}{c} \tilde{\mathbf{j}}. \end{cases} \quad (2.2)$$

Instead of using the current density \mathbf{j} , it is sometimes more convenient to deal with the polarization \mathbf{P} from the following relation

$$\mathbf{j}(\mathbf{r}, t) = \frac{\partial \mathbf{P}(\mathbf{r}, t)}{\partial t}$$

or in terms of the Fourier transform

$$\tilde{\mathbf{j}}(\mathbf{r}, \omega) = -i\omega \tilde{\mathbf{P}}(\mathbf{r}, \omega). \quad (2.3)$$

From Eqs. (2.2) and (2.3), we get

$$\nabla \times \nabla \times \tilde{\mathbf{E}} - q^2 \tilde{\mathbf{E}} = 4\pi q^2 \tilde{\mathbf{P}}, \quad (2.4)$$

where $q = \omega/c$ is the wave number in vacuum.

For the nonlocal response, we consider the induced linear optical polarization given by

$$\tilde{\mathbf{P}}(\mathbf{r}, \omega) = \int d\mathbf{r}' \chi(\mathbf{r}, \mathbf{r}', \omega) \cdot \tilde{\mathbf{E}}(\mathbf{r}', \omega), \quad (2.5)$$

where χ is the electric susceptibility tensor.

Now the general Hamiltonian for an assemble of charged particles in a given EM field described in (2.26) takes the form

$$H_M = H_0 + H_{int},$$

which is written as the sum of the Hamiltonian H_0 for the matter system and an interaction Hamiltonian, H_{int} , which describes the interaction of the matter with the electromagnetic field. Usually, we take them to be the following forms [8]

$$\begin{aligned} H_0 &= \sum_l \left\{ \frac{1}{2m_l} \mathbf{p}_l^2 + V(\mathbf{r}_l) \right\}, \\ H_{int} &= - \sum_l e_l \mathbf{r}_l \cdot \mathbf{E}(\mathbf{r}_l, t), \end{aligned} \quad (2.6)$$

where e_l , m_l , \mathbf{r}_l and \mathbf{p}_l are the charge, mass, coordinate and conjugate momentum of the coordinate, respectively, for the l th particle, $V(\mathbf{r}_l)$ is the Coulomb interaction of charged particles. We assume that $\mathbf{E}(\mathbf{r}, t)$ can be represented as a discrete sum of (positive and negative) frequency component as

$$\mathbf{E}(\mathbf{r}, t) = \sum_{\omega} \tilde{\mathbf{E}}(\mathbf{r}, \omega) \exp(-i\omega t).$$

So (2.6) can also be written as $-\sum_{\omega} \int d\mathbf{r} \hat{\mathbf{P}}(\mathbf{r}) \cdot \tilde{\mathbf{E}}(\mathbf{r}, t) \exp(-i\omega t)$, where

$$\hat{\mathbf{P}}(\mathbf{r}) = \sum_l e_l \mathbf{r}_l \delta(\mathbf{r} - \mathbf{r}_l)$$

is the electric dipole moment operator.

Consequently, the time evolution of matter state is described by the Schrödinger equation [27]

$$i\hbar \frac{\partial}{\partial t} |\psi(t)\rangle = (H_0 + H_{int}) |\psi(t)\rangle. \quad (2.7)$$

The matter state prepared at time $t = t_0$ as an eigenstate of H_0 will experience time evolution after switching on the radiation-matter interaction.

The susceptibility tensor with respect to the induced polarization can be derived from the conventional time-dependent perturbation theory. By introducing

$$|\hat{\psi}(t)\rangle = \exp(iH_0 t/\hbar) |\psi(t)\rangle,$$

Eq. (2.7) can be rewritten as

$$i\hbar \frac{\partial}{\partial t} |\hat{\psi}(t)\rangle = \hat{H} |\hat{\psi}(t)\rangle \quad (2.8)$$

with $\hat{H} = \exp(iH_0t/\hbar) H_{int} \exp(-iH_0t/\hbar)$.

Solving Eq. (2.8) up to the first-order of \hat{H} , we have

$$|\hat{\psi}(t)\rangle = |\hat{\psi}(-\infty)\rangle - \frac{i}{\hbar} \int_{-\infty}^t d\tau \hat{H}(\tau) |\hat{\psi}(-\infty)\rangle.$$

By assuming that the matter is in the ground state $|g\rangle$ at $t = -\infty$, the first-order perturbed states are given by

$$\begin{aligned} |\hat{\psi}(t)\rangle &= |g\rangle - \frac{i}{\hbar} \int_{-\infty}^t d\tau \sum_{\xi} |\xi\rangle \langle \xi| e^{iH_0\tau/\hbar} \left[- \sum_{\omega} \int d\mathbf{r}' \hat{\mathbf{P}}(\mathbf{r}') \cdot \tilde{\mathbf{E}}(\mathbf{r}') e^{-i\omega\tau} \right] e^{-iH_0\tau/\hbar} |g\rangle \\ &= |g\rangle - \frac{i}{\hbar} \sum_{\omega} \sum_{\xi} |\xi\rangle \int_{-\infty}^t d\tau e^{i(E_{\xi}/\hbar - \omega - i\gamma/\hbar)\tau} \langle \xi| \left[- \int d\mathbf{r}' \hat{\mathbf{P}}(\mathbf{r}') \cdot \tilde{\mathbf{E}}(\mathbf{r}') \right] |g\rangle \\ &= |g\rangle - \sum_{\omega} \sum_{\xi} |\xi\rangle \frac{\langle \xi| - \int d\mathbf{r}' \hat{\mathbf{P}}(\mathbf{r}') \cdot \tilde{\mathbf{E}}(\mathbf{r}') |g\rangle}{E_{\xi} - \hbar\omega - i\gamma} e^{i(E_{\xi}/\hbar - \omega - i\gamma/\hbar)t}, \end{aligned}$$

where a factor $\exp(\gamma\tau/\hbar)$, with $\gamma \rightarrow 0^+$, is introduced to indicate that at time $t_0 \rightarrow -\infty$, the perturbation H_{int} is turned on adiabatically. This factor serves mainly the purpose of keeping the derivation of all mathematical quantities properly behaved, i.e., non-singular. Here, E_{ξ} indicates the eigenenergy of excited state $|\xi\rangle$ measured from that of the ground state $|g\rangle$.

The expectation value of the polarization can be calculated as

$$\begin{aligned} \mathbf{P}(\mathbf{r}, t) &= \langle \hat{\psi}(t) | e^{iH_0t/\hbar} \hat{\mathbf{P}}(\mathbf{r}) e^{-iH_0t/\hbar} | \hat{\psi}(t) \rangle \\ &= - \sum_{\omega} \sum_{\xi} \langle g | \hat{\mathbf{P}}(\mathbf{r}) | \xi \rangle \frac{\langle \xi | - \int d\mathbf{r}' \hat{\mathbf{P}}(\mathbf{r}') \cdot \tilde{\mathbf{E}}(\mathbf{r}') | g \rangle}{E_{\xi} - \hbar\omega - i\gamma} e^{-i\omega t} e^{(\gamma/\hbar)t} \\ &\quad - \sum_{\omega} \sum_{\xi} \langle \xi | \hat{\mathbf{P}}(\mathbf{r}) | g \rangle \frac{\langle g | - \int d\mathbf{r}' \hat{\mathbf{P}}(\mathbf{r}') \cdot \tilde{\mathbf{E}}(\mathbf{r}') | \xi \rangle}{E_{\xi} - \hbar\omega + i\gamma} e^{i\omega t} e^{(\gamma/\hbar)t}. \end{aligned}$$

Then the Fourier component $\tilde{\mathbf{P}}(\mathbf{r})$ may be written as

$$\begin{aligned} \tilde{\mathbf{P}}(\mathbf{r}) &= \sum_{\xi} \langle g | \hat{\mathbf{P}}(\mathbf{r}) | \xi \rangle \frac{\langle \xi | \int d\mathbf{r}' \hat{\mathbf{P}}(\mathbf{r}') \cdot \tilde{\mathbf{E}}(\mathbf{r}') | g \rangle}{E_{\xi} - \hbar\omega - i\gamma} \\ &\quad + \sum_{\xi} \langle \xi | \hat{\mathbf{P}}(\mathbf{r}) | g \rangle \frac{\langle g | \int d\mathbf{r}' \hat{\mathbf{P}}(\mathbf{r}') \cdot \tilde{\mathbf{E}}(\mathbf{r}') | \xi \rangle}{E_{\xi} + \hbar\omega + i\gamma}. \end{aligned} \quad (2.9)$$

By ignoring the second term of Eq. (2.9) that corresponds to the antiresonant part, the induced polarization takes the form

$$\tilde{\mathbf{P}}(\mathbf{r}) = \int d\mathbf{r}' \chi(\mathbf{r}, \mathbf{r}'; \omega) \cdot \tilde{\mathbf{E}}(\mathbf{r}', \omega)$$

with $\chi(\mathbf{r}, \mathbf{r}'; \omega)$ being the susceptibility tensor

$$\chi(\mathbf{r}, \mathbf{r}'; \omega) = \sum_{\xi} \frac{\langle g | \hat{\mathbf{P}}(\mathbf{r}) | \xi \rangle \langle \xi | \hat{\mathbf{P}}(\mathbf{r}') | g \rangle}{E_{\xi} - \hbar\omega - i\gamma}.$$

In the case of bulk materials, the center of mass-motion of the exciton is approximately represented by a plane wave [1]

$$\langle g | \hat{\mathbf{P}}(\mathbf{r}) | \xi \rangle = \frac{\boldsymbol{\mu}}{\sqrt{V}} \exp(i\mathbf{k} \cdot \mathbf{r}), \tag{2.10}$$

where ξ represents the exciton state with the wave vector \mathbf{k} , V is the volume of the medium, and $\boldsymbol{\mu}$ is the intensity of induced polarization obtained from the bulk limit, $\boldsymbol{\mu}^2 = \epsilon_{bg} \Delta_{LT} / (4\pi)$, and Δ_{LT} is the splitting energy of longitudinal and transverse mode of exciton, ϵ_{bg} is the background dielectric constant.

From (2.10), it follows that

$$\chi(\mathbf{r}, \mathbf{r}') = \frac{\boldsymbol{\mu}^2}{V} \sum_{\mathbf{k}} \frac{e^{i\mathbf{k} \cdot (\mathbf{r} - \mathbf{r}')}}{E_{\mathbf{k}} - \hbar\omega - i\gamma} = \chi(\mathbf{r} - \mathbf{r}'). \tag{2.11}$$

When the valence and conduction bands are both parabolic in the \mathbf{k} -region, the energy of the exciton may be further given by

$$E_{\mathbf{k}} = E_0 + \frac{\hbar^2 \mathbf{k}^2}{2M},$$

where $E_0 = \hbar\omega_0$, and M is the mass of the exciton.

Next, define the Fourier component in the \mathbf{k} -space of the susceptibility

$$\chi(\mathbf{r} - \mathbf{r}') = \frac{1}{\sqrt{V}} \sum_{\mathbf{k}} e^{i\mathbf{k} \cdot (\mathbf{r} - \mathbf{r}')} \chi(\mathbf{k}).$$

Then we have

$$\chi(\mathbf{k}) = \frac{1}{\sqrt{V}} \frac{\boldsymbol{\mu}^2}{E_0 + \frac{\hbar^2 \mathbf{k}^2}{2M} - \hbar\omega - i\gamma}.$$

Since the polarization induced by the exciton is of the form (2.5), we can rewrite this relation in the \mathbf{k} -space as

$$\begin{aligned} \frac{1}{\sqrt{V}} \sum_{\mathbf{k}} \mathbf{P}(\mathbf{k}) &= \int d\mathbf{r}' \frac{1}{\sqrt{V}} \sum_{\mathbf{k}'} e^{i\mathbf{k}' \cdot \mathbf{r}'} E_{\omega}(\mathbf{k}') \cdot \frac{1}{\sqrt{V}} \sum_{\mathbf{k}} e^{i\mathbf{k} \cdot (\mathbf{r} - \mathbf{r}')} \chi(\mathbf{k}) \\ &= \sum_{\mathbf{k}} e^{i\mathbf{k} \cdot \mathbf{r}} \chi(\mathbf{k}) \cdot E_{\omega}(\mathbf{k}), \end{aligned}$$

where we used the fact

$$\frac{1}{V} \int d\mathbf{r} \exp(-i\mathbf{k}' \cdot \mathbf{r}) \exp(i\mathbf{k} \cdot \mathbf{r}) = \delta_{\mathbf{k}, \mathbf{k}'}$$

Hence, $\bar{\chi}(\mathbf{k}, \omega)$ may be defined as follows:

$$\bar{\chi}(\mathbf{k}, \omega) = \sqrt{V} \chi(\mathbf{k}; \omega) = \frac{\mu^2}{E_0 + \frac{\hbar^2 \mathbf{k}^2}{2M} - \hbar\omega - i\gamma}$$

The new dielectric constant take the form

$$\begin{aligned} \epsilon(\mathbf{k}, \omega) &= \epsilon_{bg} + 4\pi \bar{\chi}(\mathbf{k}, \omega) \\ &= \epsilon_{bg} + \frac{\epsilon_{bg} \Delta_{LT}}{E_0 + \frac{\hbar^2 \mathbf{k}^2}{2M} - \hbar\omega - i\gamma}, \end{aligned} \quad (2.12)$$

which depends explicitly on the wavevector \mathbf{k} and the frequency ω . It should be noted that this dielectric constant applies to a case in which the exciton polarization and the electric field are parallel, and both perpendicular to \mathbf{k} [16]. In general, the wavevector dependence of the dielectric constant is referred to as spatial dispersion, the development of the spatial dispersion in optical spectra of excitons has in great part been due to Pekar [24]. In [16], Hopfield and Thomas did a systematical study of the effects of spatial dispersion, where a wavevector dependent susceptibility was given based on the Kramers-Konig theory; while we present a rigorous derivation of $\chi(\mathbf{k}, \omega)$ from the first principle in this paper.

In comparison, the classical dielectric theory of optical properties studies the dielectric constant depending only on the frequency. The dielectric behavior is a sum over resonances, each resonance occurring at a particular frequency. Moreover, the transport of energy is neglected by any mechanism other than electromagnetic waves. However, we are investigating the optical response of confined excitons in a nano medium, so the energy transports by excitons and the electromagnetic field are equally important. In a medium characterized by $\epsilon(\mathbf{k}, \omega)$ in (2.12), the coupling of the exciton and the electromagnetic wave gives birth to so-called polariton which can carry energy and has wavevector \mathbf{k} . One of the striking properties of this medium is the existence of multi-mode polariton waves, the dispersion relation $k^2 = \epsilon(k, \omega)(\omega/c)^2$ leads to more than one solution $k_j = k_j(\omega)$, $j = 1, 2, \dots$. This means that when the medium is irradiated with light of frequency ω , more than one waves can arise inside the medium with the same frequency but with different wavenumbers. Therefore, the need of additional boundary conditions arise naturally to handle the multi-mode waves.

2.2 Additional boundary conditions

2.2.1 Excitons in a single slab

We establish the model for the optical response of an exciton in the one-dimensional confinement and discuss some mathematical issues. Consider the light scattering depicted in

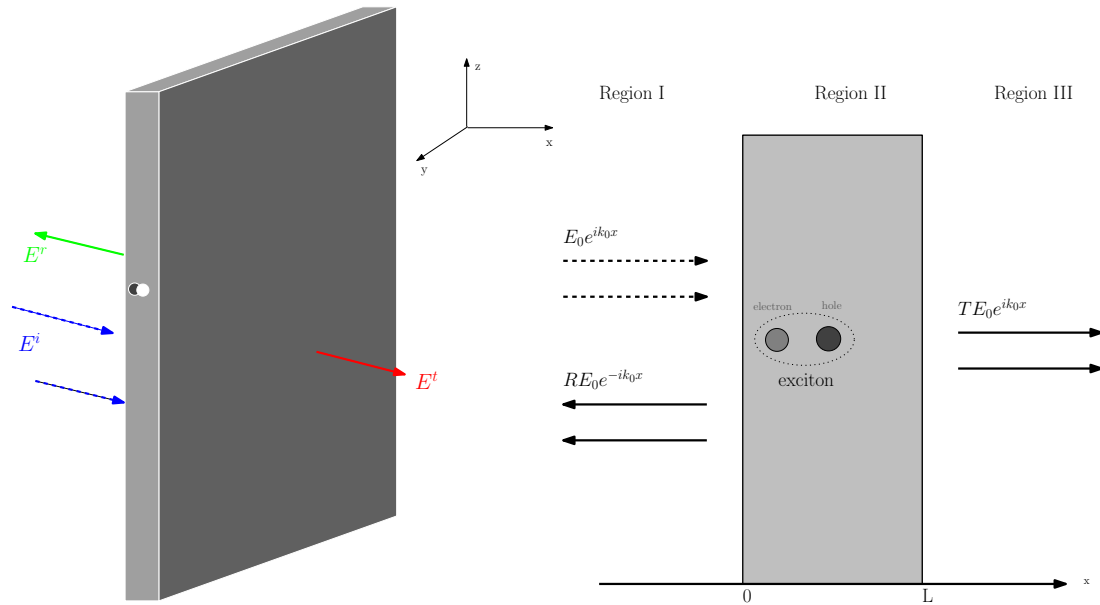


Figure 1: An exciton confined in a thin CuCl slab. Left: the full view; Right: the 1D confinement view.

Fig. 1 for an incident plane wave $\mathbf{E} = (0, 0, E_z(x))$ from the left. The background dielectric constants inside and outside the slab are denoted by ϵ_{bg} and ϵ_0 , respectively.

Maxwell's equations for the electric field inside the slab take the form

$$\nabla \times \nabla \times \mathbf{E} - \epsilon(k, \omega) q^2 \mathbf{E} = 0,$$

which may be further reduced to the Helmholtz equation

$$\nabla^2 E_z + \epsilon(k, \omega) q^2 E_z = 0$$

if the electric field is divergence free, $\nabla \cdot \mathbf{E} = 0$.

The dielectric constant $\epsilon(k, \omega)$, (2.12) and relation $k^2 = \epsilon(k, \omega) q^2$ give us

$$k^4 + \left[\frac{2M}{\hbar} (\omega_0 - \omega - i\gamma) - \epsilon_{bg} q^2 \right] k^2 - \epsilon_{bg} q^2 \frac{2M}{\hbar} (\omega_0 - \omega - i\gamma + \Delta_{LT} / \hbar) = 0, \quad (2.13)$$

which provides the dispersion relation of polariton inside the slab.

Due to the k -dependence, Eq. (2.13) has more solutions than the case of k -independent dielectric constant $\epsilon(\omega)$. For example, in the case of a simple exciton with a finite translational mass, there are generally two allowed modes of polariton for a fixed frequency ω , polarization and a given direction of propagation at the interface of the semiconductor with a spatially non-dispersive medium (vacuum, for example). In this case, additional boundary conditions (ABC) must be introduced [24], since the number of the waves at the interface is, for a given frequency, larger than that of Maxwell's boundary conditions (MBC) from the continuity of the tangential components of EM fields.

It can be verified that Eq. (2.13) has no real roots but rather four complex solutions $k_a, -k_a, k_b, -k_b$. Moreover, the solutions having positively imaginary part are physically meaningful and acceptable, which are denoted by k_a and k_b . Let the electric fields at k_a and k_b be E_a and E_b , respectively. Then the field inside the slab is given by $E_z(x) = E_a + E_b$.

The Maxwell equations for E_a and E_b are

$$\frac{d^2 E_a}{dx^2} + k_a^2 E_a = 0, \quad \frac{d^2 E_b}{dx^2} + k_b^2 E_b = 0. \quad (2.14)$$

As illustrated in Fig. 1, the incident field in Region I is $E_0 e^{ik_0 x}$, the reflected field in Region I is $RE_0 e^{-ik_0 x}$, the transmitted field in Region III is $TE_0 e^{ik_0 x}$ where $k_0 = \sqrt{\epsilon_0} q$. Then the electric field in Region I is $E_0 e^{ik_0 x} + RE_0 e^{-ik_0 x}$, where R and T are the corresponding reflectance and transmission coefficients to be determined.

The solutions of Eq. (2.14) are

$$\begin{aligned} E_a(x) &= A e^{ik_a x} + B e^{-ik_a x}, \\ E_b(x) &= C e^{ik_b x} + D e^{-ik_b x}, \end{aligned}$$

where A, B, C and D are unknowns.

All the unknowns should be determined by the boundary conditions at the sides of the slab $x=0$ and $x=L$. There are four boundary conditions from the usual Maxwell continuity conditions of the tangential components of EM fields and their derivatives. Two ABCs are obtained from the requirement that the excitonic polarization should vanish at two sides of the slab

$$P(x=0) = P(x=L) = 0.$$

It is through the two additional boundary conditions that the notion of quantization of excitons is introduced. The notion originally suggested by Pekar has often been used in the interpretation of excitonic reflectivity spectra of bulk semiconductors.

Maxwell's boundary conditions. The derivative of $E_z(x)$ in the region I is given by:

$$\begin{aligned} \frac{dE_z(x)}{dx} &= ik_0 E_0 e^{ik_0 x} - ik_0 R E_0 e^{-ik_0 x} \\ &= -ik_0 E_z(x) + 2ik_0 E_0 e^{ik_0 x}. \end{aligned}$$

Some simple calculation leads to the MBC at $x=0$

$$\left. \frac{dE_a}{dx} \right|_{x=0} + \left. \frac{dE_b}{dx} \right|_{x=0} = -ik_0 (E_a(0) + E_b(0)) + 2ik_0 E_0. \quad (2.15)$$

Similarly, from the electric field in the region III given by

$$E_z(x) = TE_0 e^{ik_0 x}$$

and its derivative

$$\frac{dE_z(x)}{dx} = ik_0TE_0e^{ik_0x} = ik_0E_z(x),$$

we can easily derive the MBC at $x = L$

$$\frac{dE_a}{dx}|_{x=L} + \frac{dE_b}{dx}|_{x=L} = ik_0(E_a(L) + E_b(L)). \tag{2.16}$$

Additional boundary conditions. $P(x=0) = P(x=L) = 0$ or equivalently

$$\chi(k_a, \omega)E_a(0) + \chi(k_b, \omega)E_b(0) = 0, \tag{2.17}$$

$$\chi(k_a, \omega)E_a(L) + \chi(k_b, \omega)E_b(L) = 0. \tag{2.18}$$

From (2.17) and (2.18), $E_b(0)$ and $E_b(L)$ can be expressed in terms of $E_a(0)$ and $E_a(L)$ as follows

$$E_b(0) = -\chi E_a(0), E_b(L) = -\chi E_a(L) \tag{2.19}$$

with $\chi = \chi(k_a, \omega) / \chi(k_b, \omega)$. Combining above boundary conditions, we obtain a simple matrix equation

$$\mathbf{M}(\omega)\mathbf{U} = \mathbf{b} \tag{2.20}$$

with

$$\mathbf{M}(\omega) = \begin{pmatrix} k_a+k_0 & k_0-k_a & k_b+k_0 & k_0-k_b \\ W(k_a-k_0) & -\frac{k_a+k_0}{W} & V(k_b-k_0) & -\frac{k_b+k_0}{V} \\ \chi & \chi & 1 & 1 \\ W\chi & \frac{\chi}{W} & V & \frac{1}{V} \end{pmatrix},$$

where $W = e^{ik_aL}$ and $V = e^{ik_bL}$, L is the thickness of the slab. Note that every element in the matrix depends on the incident frequency ω . Here $\mathbf{U} = (A, B, C, D)^T$, $\mathbf{b} = (2k_0E_0, 0, 0, 0)^T$.

It is easily verified that

$$\begin{aligned} \det(\mathbf{M}(\omega)) = & -\frac{1}{WV} \left[k_a+k_0 - \chi(k_0+k_b) \right]^2 + \frac{W}{V} \left[k_a-k_0 + \chi(k_0+k_b) \right]^2 \\ & - WV \left[k_a-k_0 - \chi(k_b-k_0) \right]^2 + \frac{V}{W} \left[k_a+k_0 + \chi(k_b-k_0) \right]^2 - 8\chi k_a k_b, \end{aligned}$$

which is a quadratic form of χ .

If χ is regarded as an unknown, then we will have two roots of $\det(\mathbf{M}) = 0$:

$$\chi_1 = \frac{(V-1)[k_0(W-1) - k_a(W+1)]}{(W-1)[k_0(V-1) - k_b(V+1)]}, \tag{2.21}$$

$$\chi_2 = \frac{(V+1)[k_0(W+1) - k_a(W-1)]}{(W+1)[k_0(V+1) - k_b(V-1)]}. \tag{2.22}$$

Therefore, the linear system (2.20) should always have a unique solution if neither (2.21) nor (2.22) is satisfied.

Theorem 2.1. *In the resonance region, the system (2.20) has a unique solution.*

It should be noted that the optical resonance is expected to happen at around $E_\omega = \hbar\omega_0$ when the exciton state is prepared. It is thus natural to consider a small energy region around $\hbar\omega_0$, or a small perturbation of the incident energy E_ω by $\delta(\omega)$. In addition, we are interested in what happens when the EM field entering into the resonance region of a material, and through analyzing the computational results, we can, for example, adjust the frequency of incident field, the size or shape of the material to achieve maximal yields, which is an optimal design problem.

Proof. Denote $\delta(\omega) = E_\omega - \hbar\omega_0$. When $\delta(\omega) = 0$ or the frequency of the incident light is the same as that of the exciton, we can get two modes k_a^0 and k_b^0 by solving Eq. (2.13). For the CuCl semiconductor slab, it is easily calculated that

$$\det\mathbf{M}(\omega_0) = -0.3451977257e-5 + 0.1774810304ie-5.$$

After some tedious calculation, we can expand $\det\mathbf{M}(\omega)$ around ω_0 as

$$\det\mathbf{M}(\omega) = \det\mathbf{M}(\omega_0) + a\delta + b\delta^2 + \mathcal{O}(\delta^3),$$

where $a \approx -7.377 - 14.2354i$ and $b \approx -2.35e6 - 2.07ie6$. Therefore, for δ small enough, the matrix $\mathbf{M}(\omega)$ is nonsingular and hence there is a unique solution of Eq. (2.20). \square

2.2.2 Excitons in a square

To study the two-dimensional confinement effect of excitons, we discuss a case where a CuCl square is inserted between two parallel perfect conductors (waveguide); see the geometry in Fig. 2, a similar geometry was studied in [18]. For simplicity, we assume the background is filled with a homogeneous medium. Due to the discontinuity—both material and excitons—the CuCl square can only transmit part of the incident field, some part of the field will be reflected and will propagate in the opposite direction. It is very important to determine the reflection efficiency and transmission efficiency in devices design or microwave measurements.

Let a TE field $\mathbf{E} = (0, 0, E_z)$ be incident on the waveguide from the left. Far left to the CuCl square, the total electric field can be expressed as a sum of the incident field and reflected field:

$$E_z = E_z^{inc} + E_z^{ref} = E_0 e^{ik_0 x} + R E_0 e^{-ik_0 x}, \quad (2.23)$$

where E_0 is a constant and R is the reflection coefficient. Far right to the square,

$$E_z = E_z^{tran} = T E_0 e^{ik_0 x}, \quad (2.24)$$

where T is the transmission coefficient. Here both R and T are to be determined.

The governing equation is:

$$\nabla^2 E_z + k^2 E_z = 0 \quad (2.25)$$

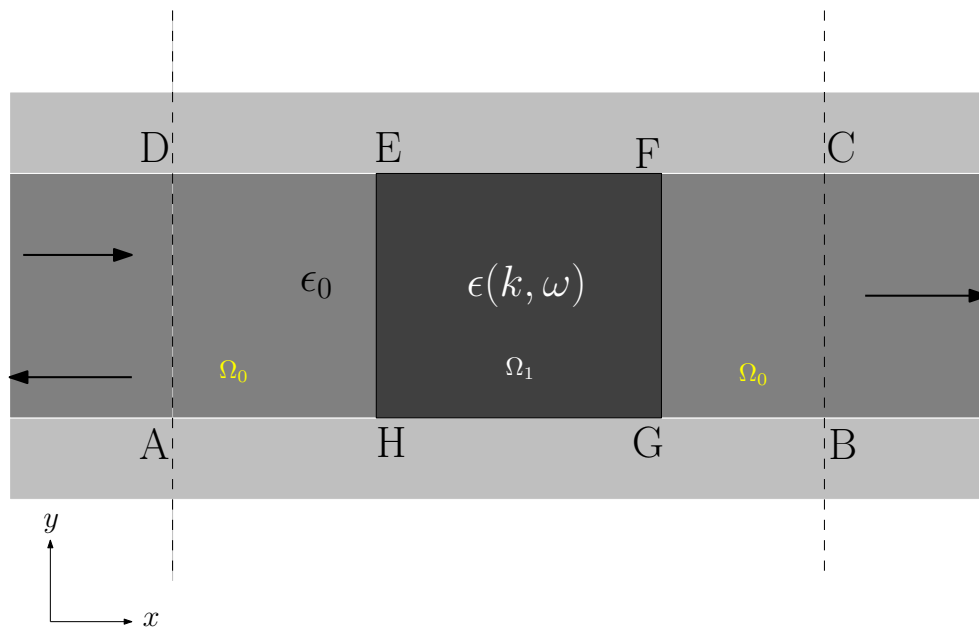


Figure 2: A CuCl square inserted in a parallel-plate waveguide.

with

$$k = \begin{cases} k_a, k_b & \Omega_1, \\ k_0 & \Omega_0. \end{cases} \tag{2.26}$$

And we have $E_z = E_a + E_b$ in Ω_1 since there are two waves existing inside the CuCl square.

As the wall of the waveguide is assumed to be perfect conductor, there cannot be an electric field inside. Hence, in the wall, the electric field must vanish. Then we have Dirichlet boundaries $E_z = 0$ along the walls by the continuity of the tangential component of E .

At the interface EH and FG, we impose the additional boundary conditions

$$\chi(k_a, \omega)E_a + \chi(k_b, \omega)E_b = 0$$

as well as the jump conditions

$$E_z = E_a + E_b, \quad \frac{\partial E_z}{\partial n} = \frac{\partial(E_a + E_b)}{\partial n}.$$

In order to apply numerical methods to compute the problem, we must reduce or truncate the infinite domain into a finite domain. Accordingly, we introduce two artificial boundaries AD and BC. If AD is far enough from EH (at least one wavelength), then the

field can be approximated by (2.23). Therefore, we get

$$\begin{aligned}\frac{\partial E_z}{\partial n} &\approx ik_0 E_0 e^{ik_0 x} - ik_0 R E_0 e^{-ik_0 x} \\ &= ik_0 E_z - 2ik_0 E_0 e^{ik_0 x},\end{aligned}$$

which can be used as the boundary condition on AD. Similarly, we can take $\frac{\partial E_z}{\partial n} \approx ik_0 E_z$ as the boundary condition on BC.

Once we finish solving Eq. (2.25) along with the boundaries, we can obtain R and T from (2.23) and (2.24)

$$R = \frac{E_z(x_1) - E_0 e^{ik_0 x_1}}{E_0 e^{-ik_0 x_1}}, \quad T = \frac{E_z(x_2)}{E_0 e^{ik_0 x_2}}, \quad (2.27)$$

where x_1 and x_2 are the positions of AD and BC.

3 Numerical experiments

3.1 One-dimensional confinement

We apply the semiclassical model in Section 2 to calculate the linear optical response by the exciton in a CuCl slab in the region Z_3 exciton. The following parameters are used

$$\epsilon_{bg} = 5.59, \quad \epsilon_0 = 1.0, \quad \hbar\omega_0 = 3.2022\text{eV}, \quad M = 2.3m_0, \quad \Delta_{LT} = 5.65\text{meV}, \quad \gamma = 1\text{meV},$$

where m_0 is the mass of an electron.

Fig. 3 shows the spectra of the transmitted and reflected lights by CuCl slab of different sizes. The resonant structures showed in the figures are due to the exciton mode, interfering with the size resonance of the slab. Excitons in a semiconductor slab are well studied for various thicknesses including a semi-infinite limit [9, 11, 16]. In theory, if all the multiple reflection effects are neglected, two kinds of oscillatory effects should be observed. One is periodic modulation of the transmission at fixed energy as a function of the thickness. The other is a periodic modulation of the transmission at fixed thickness as a function of the energy. Both these two effects are clearly verified in our numerical experiments. Compared with the normal incidence reflection experiments in CdS [11], the experimental line shape, especially the resonance peaks are well produced. Also from Fig. 3, the peaks of spectral transmission and reflection clearly indicate enhanced optical absorptions, and those peaks move to the right as the CuCl slab thickness decreases, which is the well known **blue shift** phenomenon.

3.2 Two-dimensional confinement

For the two-dimensional confinement, according to (2.27), reflection and transmission coefficients are calculated by using a finite difference scheme (5-point stencil) for the

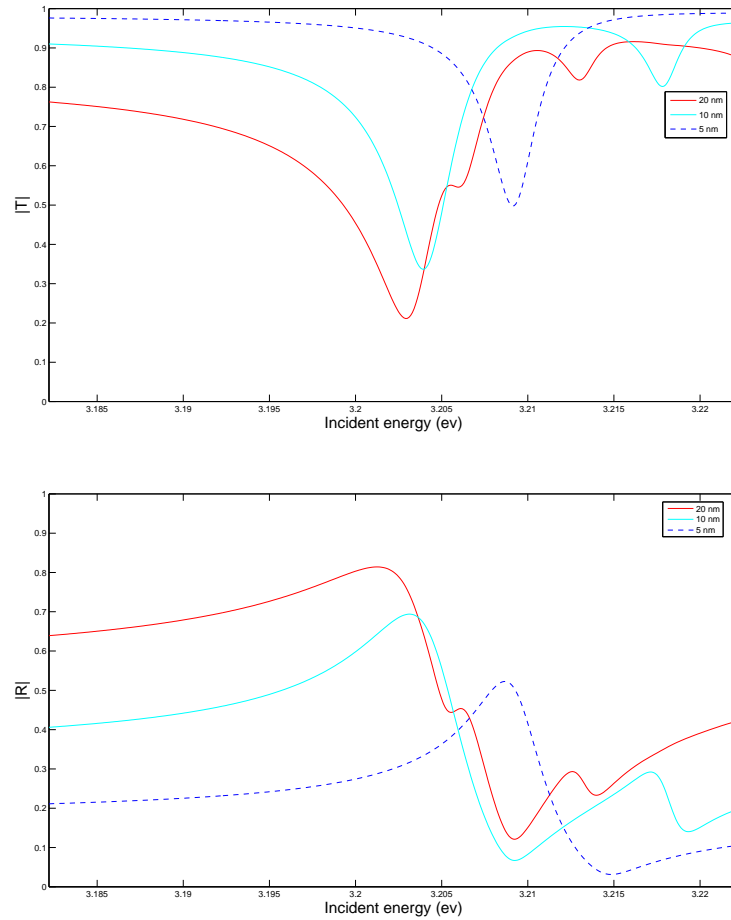


Figure 3: Size dependence of spectral transmission and reflection of the CuCl slab. The horizontal axis is the incident energy (eV). Top: transmission spectrum; Bottom: reflection spectrum.

Laplace operator to discretize the Helmholtz equations (2.25) and boundary conditions. Due to the confined exciton, the optical response of the CuCl square depends resonantly on the size and light frequency, which is clearly showed in Fig. 4. For $L = 10$ nm, peaks happening around the frequency $\hbar\omega = 3.2022\text{eV}$ indicates that there is an absorption enhancement at around $\hbar\omega = 3.2022\text{eV}$, which is the exact amount of energy required to produce an exciton in the CuCl square. As a comparison, a similar problem was studied in [18] where the author considered a TM field and only one wave inside the Ω_1 (no additional boundary conditions). For fixed incident energy, R and T were computed via a finite element approach for various sizes of Ω_1 . For our case, we are more interested in observing the effect of spatial resonance dispersion on optical properties near exciton absorption peaks which are attractive to investigate, and we believe our numerical results are quite trustable in capturing those resonant peaks.

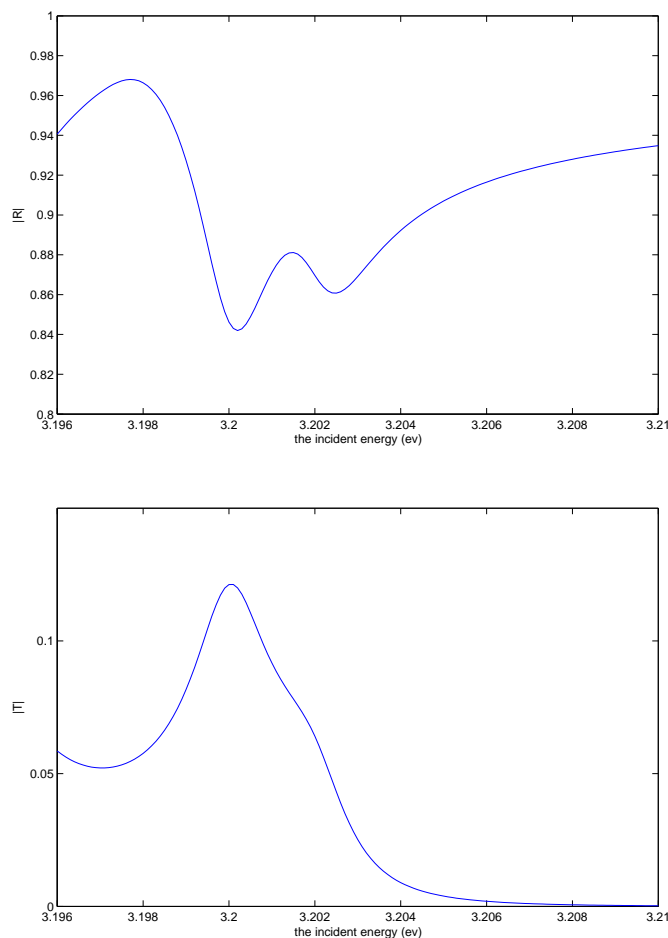


Figure 4: The reflection spectrum (top) and transmission spectrum (bottom) of the CuCl square ($L = 10\text{nm}$). The horizontal axis is the incident energy (eV).

4 Concluding remarks

Based on Cho's original nonlocal response theory, a new semiclassical model is developed to describe the exciton effects in the microscopic semiconductor. In the weak confinement regime, for the linear response, a spatially dispersive dielectric constant is derived from the first principle. To compute the confinement effect of an exciton in microscopic semiconductors of different shapes, we impose "no excitonic polarization" conditions at the interface of the semiconductor and surrounding medium, and for the first time we analyze and compute the two-dimensional confinement of the exciton. Currently, we are investigating three-dimensional confinement effects in the nonlinear response regime, in particular, excitons and interaction of excitons in a three-dimensional

microscopic medium. Mathematically, little is known about the models. Another ongoing project is to investigate the well-posedness of the model partial differential equations in the two-dimensional case.

Acknowledgments

The research of G. Bao and Y. Sun was supported in part by the NSF grants DMS-0604790 CCF-0514078, and EAR-0724527, the ONR grant N000140210365, and the National Science Foundation of China grant 10428105.

References

- [1] H. Ajiki and K. Cho, *Longitudinal and transverse components of excitons in a spherical quantum dot*, Phys. Rev. B, 62 (2000), pp. 7402-7412.
- [2] G. Bao and Y. Chen, *A nonlinear grating problem in diffractive optics*, SIAM J. Math. Anal., Vol. 28, No. 2 (1997), pp. 322-337.
- [3] G. Bao and D. Dobson, *Second harmonic generation in nonlinear optical films*, J. Math. Phys., 35 (1994), pp. 1622-1633.
- [4] G. Bao and D. Dobson, *Diffractive optics in nonlinear media with periodic structures*, European J. Appl. Math., 6 (1995), pp. 573-590.
- [5] G. Bao and P. Li, *Inverse medium scattering problems in near-field optics*, J. Comp. Math., 25 (2007), pp. 252-265.
- [6] F. Bassani, G.C. La Rocca, and M. Artoni, *Electromagnetic induced transparency in bulk and microcavity semiconductors*, J. Lum., 110 (2004), pp. 174-180.
- [7] M. Born and K. Huang, *Dynamical Theory of Crystal Lattice*, Clarendon Press, Oxford, 1954.
- [8] R.W. Boyd, *Nonlinear Optics*, Academic Press, San Diego, 2003.
- [9] K. Cho, *Optical Response of Nanostructures : Microscopic Nonlocal Theory*, Springer, New York, 2003.
- [10] C. Cohen-Tannoudji, J. Dupont-Roc, and G. Grynberg, *Photons and Atoms : Introduction to Quantum Electrodynamics*, Wiley, New York, 1989.
- [11] A. D'Andrea and R. Del Sole, *Wannier-Mott excitons in semi-infinite crystals: Wave functions and normal-incidence reflectivity*, Phys. Rev. B, 25 (1982), pp. 3714-3730.
- [12] M. S. Dresselhaus, G. Dresselhaus, R. Saito, and A. Jorio, *Exciton photophysics of carbon nanotubes*, Annu. Rev. Phys. Chem., 58 (2007), pp. 719-747.
- [13] G. Grosso and G. P. Parravicini, *Solid State Physics*, Academic Press, San Diego, 2003.
- [14] T. Hagstrom and S. Lau, *Radiation boundary conditions for Maxwell's equations: A review of accurate time-domain formulations*, J. Comp. Math., 25 (2007), pp. 305-336.
- [15] E. Hanamura, *Very large optical nonlinearity of semiconductor microcrystallites*, Phys. Rev. B, 37 (1988), pp. 1273-1279.
- [16] J.J. Hopfield and D.G. Thomas, *Theoretically and experimental effects of spatial dispersion on the optical properties of crystal*, Phys. Rev., 132 (1963), pp. 563-572.
- [17] A.M. Janner, *Second Harmonic Generation, a Selective Probe for Excitons*, Ph.D. Thesis, University of Groningen, Groningen, Netherlands, 1998.
- [18] J.M. Jin, *The finite element method in electromagnetics*, Wiley, New York, 2002.

- [19] P. Joly, J-R Li, and S. Fliss, *Exact boundary conditions for periodic waveguides containing a local perturbation*, Commun. Comput. Phys., 1 (2006), pp. 945-973.
- [20] B.A. Joyce, P.C. Kelires, A.G. Naumovets, and D.D. Vvedensky (Eds.), *Quantum Dots : Fundamentals, Applications, and Frontiers*, Springer, New York, 2005.
- [21] O. Keller, *Local fields in the electrodynamics of mesoscopic media*, Phys. Rep., 268 (1996), pp. 85-262.
- [22] Y. Y. Lu, *Some techniques for computing wave propagation in optical waveguides*, Commun. Comput. Phys., 1 (2006), pp. 1056-1075.
- [23] Y. Masumoto, M. Yamazaki, and H. Sugawara, *Optical nonlinearities of excitons in CuCl microcrystals*, Appl. Phys. Lett., 53 (1988), pp. 1527-1529.
- [24] S.I. Pekar, *The theory of electromagnetic waves in crystal in which excitons are produced*, Sov. Phys. JETP, 6 (1958), pp. 785-796.
- [25] H. Petersson, C. Pryor, L. Landin, M.E. Pistol, N. Carlson, W. Seifert, and L. Samuelson, *Electrical and optical properties of self-assembled InAs quantum dots in InP studied by space-charge spectroscopy and photoluminescence*, Phys. Rev. B, 61 (2000), pp. 4795-4800.
- [26] M.A. Reed, *Quantum dots*, Scientific American, 268 (1993), pp. 118-123.
- [27] J.J. Sakurai and S.F. Tuan, editor, *Modern Quantum Mechanics*, Benjamin/Cummings, Menlo Park, 1985.
- [28] A. Stahl and I. Balslev, *Electrodynamics of the Semiconductor Band Edge*, Springer Tract in Mod. Phys. 110, Springer-Verlag, New York, 1987.
- [29] Z.K. Tang, A. Yanase, T. Yasui, Y. Segawa, and K. Cho, *Optical selection rule and oscillator strength of confined exciton system in CuCl thin films*, Phys. Rev. Lett., 71 (1993), pp. 1431-1434.
- [30] T. Takagahara and E. Hanamura, *Giant-Oscillator-Strength effect on excitonic optical nonlinearities due to localization*, Phys. Rev. Lett., 56 (1986), pp. 2533-2536.
- [31] D.F. Walls and G.J. Milburn, *Quantum Optics*, Springer-Verlag, New York, 1994.
- [32] F. Wang, G. Dukovic, L.E. Brus, and T.F. Heinz, *The optical resonance in carbon nanotube arise from excitons*, Science 308 (2005), pp. 838-841.
- [33] S. Yano, T. Goto, and T. Itoh, *Excitonic optical nonlinearity of CuCl microcrystals in a NaCl matrix*, J. Appl. Phys., 79 (1996), pp. 8216-8222.
- [34] P.S. Zory, Jr, *Quantum Well Lasers*, Academic Press, Boston, 1993.